

GSC 07396–00759 = V4046 Sgr C[D]: a Wide-separation Companion to the Close T Tauri Binary System V4046 Sgr AB

J. H. Kastner¹, G. G. Sacco¹, R. Montez Jr.¹, D. P. Huenemoerder², H. Shi¹, E. Alecian³, C. Argiroffi^{4,5}, M. Audard^{6,7}, J. Bouvier⁸, F. Damiani⁵, J.-F. Donati⁹, S. G. Gregory¹⁰, M. Güdel¹¹, G. A. J. Hussain¹², A. Maggio⁵, T. Montmerle¹³

ABSTRACT

We explore the possibility that GSC 07396–00759 (spectral type M1e) is a widely separated ($\sim 2.82'$, or projected separation $\sim 12,350$ AU) companion to the “old” (age ~ 12 Myr) classical T Tauri binary system V4046 Sgr AB, as suggested by the proximity and similar space motions of the two systems. If the two systems are equidistant and coeval, then GSC 07396–00759, like V4046 Sgr AB, must be a spectroscopic binary with nearly equal-mass components, and V4046 Sgr must be at least ~ 8 Myr old. Analysis of a serendipitous Chandra X-ray gratings spectrum and light curve as well as XMM-Newton light curves

¹Center for Imaging Science, Rochester Institute of Technology, 54 Lomb Memorial Drive, Rochester NY 14623 USA (jhk@cis.rit.edu)

²MIT, Kavli Institute for Astrophysics and Space Research, 77 Massachusetts Avenue, Cambridge, MA 02139, USA

³Observatoire de Paris, LESIA, 5, place Jules Janssen, F-92195 Meudon Principal Cedex, France

⁴Dip. di Fisica, Univ. di Palermo, Piazza del Parlamento 1, 90134 Palermo, Italy

⁵INAF - Osservatorio Astronomico di Palermo, Piazza del Parlamento 1, 90134 Palermo, Italy

⁶ISDC Data Center for Astrophysics, University of Geneva, Ch. d'Ecogia 16, CH-1290 Versoix, Switzerland

⁷Observatoire de Genève, University of Geneva, Ch. des Maillettes 51, 1290 Versoix, Switzerland

⁸UJF-Grenoble 1 / CNRS-INSU, Institut de Planétologie et d'Astrophysique de Grenoble (IPAG) UMR 5274, Grenoble, F-38041, France

⁹IRAP-UMR 5277, CNRS & Univ. de Toulouse, 14 Av. E. Belin, F-31400 Toulouse, France

¹⁰California Institute of Technology, MC 249-17, Pasadena, CA 91125 USA

¹¹University of Vienna, Department of Astronomy, Türkenschanzstrasse 17, 1180 Vienna, Austria

¹²ESO, Karl-Schwarzschild-Strasse 2, 85748 Garching bei München, Germany

¹³Institut d'Astrophysique de Paris, 98bis bd Arago, FR 75014 Paris, France

and CCD spectra of GSC 07396–00759 obtained during long exposures targeting V4046 Sgr AB reveals a relatively hard ($T_X \sim 10^7$ K) X-ray spectrum, strong flaring, and relatively low-density plasma. These X-ray characteristics of GSC 07396–00759 are indicative of a high level of coronal activity, consistent with its apparent weak-lined T Tauri star status. Interactions between V4046 Sgr AB and GSC 07396–00759 when the two systems were more closely bound may be responsible for (a) their dissolution $\sim 10^6$ yr ago, (b) the present tight, circular orbit of V4046 Sgr AB, and (c) the persistence of the gaseous circumbinary disk still orbiting V4046 Sgr AB.

1. Introduction

Thanks to their proximity, individual members of the various nearby ($D \lesssim 100$ pc), young (age ~ 10 – 70 Myr) stellar groups identified over the past ~ 15 yr (for a recent review, see Zuckerman et al. 2011) provide readily accessible examples of, among other things, the late evolution of protoplanetary disks (e.g., Akeson et al. 2011; Hughes et al. 2011, and references therein) and the early stages of evolution of exoplanetary systems (Marois et al. 2008) and hierarchical binary star systems (Kastner et al. 2008a). In their tests of a method to identify such comoving groups of young stars, Torres et al. (2006) established as a candidate member of the β Pic Moving Group (β PMG) the close binary classical T Tauri system V4046 Sgr ($P \sim 2.4$ d; Stempels & Gahm 2004, and references therein). Via the cluster traceback method, Torres et al. (2008) estimated a distance of only 73 pc to V4046 Sgr. Although the age of the β PMG is estimated to be ~ 12 Myr (Zuckerman & Song 2004, and references therein), the twin members of this fascinating, short-period binary are both evidently still accreting (Stempels & Gahm 2004) from a relatively large and massive circumbinary disk of gas and dust (Kastner et al. 2008b; Rodriguez et al. 2010).

Torres et al. (2006, 2008) also identified, as another β PMG candidate, the star GSC 07396–00759 (hereafter GSC0739, spectral type M1e or M1.5e; Riaz et al. 2006), on the basis of its proximity to V4046 Sgr (separation $2.82'$) and the similar radial velocities and similarly large photospheric Li abundances of the two systems (the Li $\lambda 6708$ equivalent widths of V4046 Sgr and GSC0739 are 440 and 200 mÅ, respectively; Riaz et al. 2006; da Silva et al. 2009). Given the low surface density of known β PMG members, it is reasonable to hypothesize that GSC0739 is a distant (projected separation ~ 12.4 kAU) companion to the V4046 Sgr binary, as speculated by Torres et al. (2006). In this respect the relationship of GSC0739 to V4046 Sgr may be very much like that of 2M1235-39 to the well-studied TW Hya Association (TWA) system HR 4796AB (Kastner et al. 2008a), whose primary is a young (β

Pic-like) A star with debris disk, or that of the brown dwarf candidate TWA 28 to TW Hya itself (Teixeira et al. 2008).

If GSC0739 and 2M1235-39 (= HR 4796C, the putative tertiary component of HR 4796) are distant companions to the better-studied V4046 Sgr and HR 4796, respectively, then their present orbital periods are $\sim 10\%$ of the (~ 10 Myr) ages of these systems. Hence these objects may offer unique insight into the orbital evolution (and especially the dissolution) of young hierarchical binaries and, perhaps, the likelihood of, and conditions necessary for, formation of planets with circumbinary vs. circumstellar orbits.

Here, we briefly evaluate the available data concerning the space motions of V4046 Sgr and GSC0739, and we analyze optical/IR photometry and serendipitous X-ray observations of GSC0739 (including new XMM-Newton X-ray data obtained during the course of a coordinated observing campaign targeting V4046 Sgr; Argiroffi et al. 2011). We use the results to assess the likelihood that GSC0739 is indeed a distant companion to V4046 Sgr and to better ascertain the nature of the former. Finally, we consider the implications if the two systems are (or were) physically bound.

2. Data, Analysis, and Results

2.1. Proper motions and radial velocities

The UCAC3 catalog (Zacharias et al. 2010) proper motions (PMs) listed for V4046 Sgr and GSC0739 are $(\mu_\alpha, \mu_\delta) = (+3.3 \pm 1.7, -52.0 \pm 1.3)$ mas yr $^{-1}$ and $(+1.1 \pm 2.8, -40.0 \pm 13.6)$ mas yr $^{-1}$, respectively, indicating that (given the UCAC3 measurement errors) the PMs of the two systems are indistinguishable¹. The heliocentric radial velocities (V_{helio}) of the two systems are also very similar: Torres et al. (2006) list $V_{\text{helio}} = -5.7$ km s $^{-1}$ for GSC0739, and CO radio line measurements yield $V_{\text{helio}} = -6.2 \pm 0.2$ km s $^{-1}$ for V4046 Sgr AB (Kastner et al. 2008b; Rodriguez et al. 2010)².

¹The identical PMs listed for the two systems by Torres et al. (2006, their Table 6) both correspond to the Tycho catalog PM of V4046 Sgr AB, i.e., $(+2.1 \pm 2.1, -54.5 \pm 2.3)$ mas yr $^{-1}$; there is no Tycho catalog listing for GSC0739.

²Recent results from high-resolution optical spectroscopy indicate that the systemic velocity of V4046 Sgr AB may vary by ~ 0.5 km s $^{-1}$ (Donati et al. 2011).

2.2. Optical/IR SED and comparison with pre-MS tracks

By matching Kurucz model atmospheres (Kurucz 1993) appropriate for late-type main sequence stars (i.e., $\log g = 4.5$) to optical/near-IR photometry available in SIMBAD³ for GSC0739 (Table 1), we deduce a photospheric effective temperature 3500 ± 100 K, consistent with the M1–1.5 spectral type previously determined for GSC0739 (Torres et al. 2006; Riaz et al. 2006). From the Kurucz model normalization, and assuming the distance to GSC0739 is 73 pc (i.e., that GSC0739 and V4046 Sgr are equidistant), we determine a bolometric luminosity $L_{\text{bol}} = 0.15 L_{\odot}$ (with an approximate uncertainty, dominated by the uncertainty in distance, of $\sim 25\%$). This estimate is consistent with that obtained from the J magnitude and V–K color of GSC0739, $L_{\text{bol}} = 0.17 L_{\odot}$, following the method described in Kenyon & Hartmann (1995).

We used the foregoing results for GSC0739 and adopted the luminosity and temperature results reported for the individual components of V4046 Sgr AB by Donati et al. (2011) to place these systems on theoretical pre-MS tracks (Fig. 1). The comparison illustrates that the two systems can be both equidistant and coeval only if GSC0739, like V4046 Sgr AB, consists of two components with nearly equal luminosities. Indeed, GSC0739 is flagged as a possible spectroscopic binary by Torres et al. (2006). The positions of the GSC0739 and V4046 Sgr AB systems with respect to the overlaid model evolutionary tracks indicate ages of between ~ 10 and ~ 20 Myr, if GSC0739 is a binary. This is consistent with independent (kinematic and pre-MS evolutionary track) age estimates of ~ 12 Myr for the β PMG (see review in Zuckerman & Song 2004). On the other hand, if GSC0739 is single, then Fig. 1 indicates that its age is in the range ~ 3 –10 Myr, i.e., somewhat young for a β PMG member.

2.3. X-ray light curves and spectra

An off-axis Chandra/HETGS gratings spectrum of GSC0739 (total exposure 144.6 ks; OBSIDs 5422, 6265; PI: Herczeg) was serendipitously obtained in 2005 Aug. during an observation targeting V4046 Sgr (Günther et al. 2006). The GSC0739 X-ray spectral data are uncontaminated by V4046 Sgr AB, but the spectral resolution and the exposure of the GSC0739 source are somewhat compromised by its ($\sim 3'$) off-axis position. We extracted and combined the medium-energy gratings (MEG) and high-energy gratings (HEG) spectra for the full ~ 145 ks exposure duration and generated a light curve covering the first (longer) of the two exposure segments; the resulting light curve and spectrum are displayed in Fig. 2.

³The SIMBAD database is maintained and operated at CDS, Strasbourg, France.

The total (HEG+MEG) count rate, averaged over the entire 144.6 ks exposure duration, was $0.014 \text{ counts s}^{-1}$.

XMM European Photon Imaging Camera (EPIC) data were serendipitously obtained for GSC0739 in 2009 Sept., again during an observation (3 exposures of ~ 100 ks) targeting V4046 Sgr (Argiroffi et al. 2011). As the source fell along a bad column of EPIC’s pn detector, we only analyzed data from the two MOS detectors (the source also fell near the edge of the active area of MOS1, but these data were only slightly compromised). We used the XMM Scientific Analysis System (SAS⁴ version 10.0.0) to extract MOS1 and MOS2 light curves for the full (~ 5 day) duration of the 3×100 ks exposure (top panel of Fig. 3) as well as MOS1 and MOS2 CCD spectra and responses for each individual ~ 100 ks exposure interval (bottom panels of Fig. 3). Calibrations were performed using the current calibration files (CCF) from release note 271, 21-Dec-2010. Combined MOS1+MOS2 count rates are listed in Table 2.

The Chandra and XMM light curves reveal strong X-ray flaring at GSC0739. An impulsive flare with amplitude ~ 10 times the quiescent flux level and exponential decay is observed starting at about 65 ks into the first ~ 100 ks segment of the Chandra observation (Fig. 2, top panel). A flare of similar shape (with amplitude ~ 4 times quiescent) is observed near the beginning of the overall ~ 5 -day XMM exposure, and its decay appears to last the entire duration of the first ~ 100 ks exposure segment; a smaller flare (and several small count rate spikes) are also seen in the second and third XMM exposure segments (Fig. 3, top).

Table 2 and Fig. 3 (bottom panels) summarize the results of fits of variable-abundance (see below) absorbed two-component thermal plasma models to spectra extracted from the three ~ 100 ks XMM/EPIC (MOS) exposure intervals. A similar model fit to Chandra/HETGS data (not shown) yields similar results — i.e., a prominent hard component with $T_X \sim 20$ MK, and a weaker soft component with $T_X \sim 5\text{--}7$ MK — despite the different instrumentation; we conclude that, overall, the plasma physical conditions did not change markedly between 2005 and 2009. Nevertheless, the strong short-term variability of the source is apparent in the XMM fit results (Table 2), which indicate a steady decline in the emission measure of the hard component and, possibly, a slight decrease in T_X as the observation progressed and the strong flare faded (the source may have suffered from photon pileup during the first exposure interval).

Individual line intensities in the Chandra/HETGS data are not particularly well fit by the foregoing simple (two-component) model, as expected given the continuum of plasma temperatures that is likely present in the X-ray-emitting region. Hence, we performed global

⁴<http://xmm.esa.int/sas>

fitting of a broken power law emission measure distribution model (using *isis*⁵ and ATOMDB v2.0⁶), such as used by Rosner et al. (1978) or Peres et al. (2001) for modeling coronal loops, to the gratings data. The model is specified by an emission measure normalization, the peak temperature (T_{peak}), the power law slopes below (α) and above (β) the peak temperature, and the elemental abundances. The interstellar absorption was assumed to be negligible (a safe assumption given the very modest absorption determined from the fits to XMM data; Table 2). To account for the instrumental off-axis PSF, we used a broadening equivalent to a Gaussian turbulent velocity of 600 km s^{-1} . The resulting best fit model is overlaid on the Chandra/HETGS spectrum in Fig. 2 (bottom panel); the best-fit model parameters are $T_{peak} = 11.2 \text{ MK}$ (0.97 keV), $\alpha = 0.2$, $\beta = -1.8$, and an emission measure of $3.3 \times 10^{52} \text{ cm}^{-3}$. The best-fit abundance ratios (relative to solar) are $\text{Ne/O} = 1.8$, $\text{Mg/O} = 0.27$, $\text{Si/O} = 0.6$, and $\text{Fe/O} = 0.27$ (the two-component plasma model fits to the XMM/MOS data also indicate an elevated Ne/O ratio and depressed Fe/O ratio). These Ne/O and Fe/O ratios are typical of coronally active stars (see review in Testa 2010). Analysis of X-ray gratings spectra of V4046 Sgr AB likewise indicates enhanced Ne/O and low Fe/O, although the Ne/O enhancement is more extreme (a factor ~ 5 larger than solar; Günther et al. 2006) in the case of this (actively accreting) system.

Although the resolution of the Chandra/HETGS spectrum of GSC0739 suffers from degradation due to the off-axis position of the source, it is apparent that the forbidden to intercombination line ratio within the He-like Ne IX line complex (at $\sim 13.5 \text{ \AA}$) is large (Fig. 2, inset in bottom panel), indicative of lower-density ($\lesssim 10^{10} \text{ cm}^{-3}$) plasma. Fig. 2 (bottom panel) also illustrates the relatively large Ne X to Ne IX line ratios of GSC0739, reflecting the dominance of relatively hot ($\gtrsim 10 \text{ MK}$) plasma in its emission measure distribution (Table 2). These density- and temperature-sensitive Ne line ratios are consistent with coronal X-ray emission and, hence, a weak-lined T Tauri classification for this source (see, e.g., Kastner et al. 2004; Huenemoerder et al. 2007). Both Ne line spectral diagnostics also stand in stark contrast to those of V4046 Sgr AB; the latter displays Ne (and O) line ratios indicative of a significant emission contribution from cooler ($\sim 3 \text{ MK}$) plasma at much higher density ($\sim 10^{12} \text{ cm}^{-3}$; Günther et al. 2006, Argiroffi et al. 2011), as expected if much of the X-ray emission (essentially, all of the soft component) is generated in accretion shocks (Sacco et al. 2010, and references therein).

⁵<http://space.mit.edu/cxc/isis/>

⁶<http://www.atomdb.org/>

3. Discussion and Conclusions

The available proper motion and radial velocity data (§2.1) support the hypothesis that V4046 Sgr AB and GSC0739 are comoving systems. Hence – provided GSC0739 is also a close binary (§3.2) – the two systems likely constitute a hierarchical multiple and, in the following, we refer to GSC0739 as V4046 Sgr C[D].

3.1. The nature of V4046 Sgr C[D]

Based on its lack of $H\alpha$ emission ($H\alpha$ equivalent width of $+3.1 \text{ \AA}$; Riaz et al. 2006), V4046 Sgr C[D] appears to be best classified as a weak-lined T Tauri system (wTTS); i.e., unlike V4046 Sgr AB, the system shows no evidence for ongoing accretion. The prominent hard ($T_X \sim 10^7 \text{ K}$) X-ray spectral component, strong X-ray flaring, and relatively low-density X-ray-emitting plasma of V4046 Sgr C[D] (§2.3) — all of which are indicative of a high level of coronal activity — are fully consistent with such a wTTS classification.

3.2. V4046 Sgr AB and C[D]: constraints on system age and origin

If the V4046 Sgr AB and C[D] systems are indeed bound, they are only weakly so, given their very large projected separation of $\sim 12,350 \text{ AU}$ (assuming $D = 73 \text{ pc}$). Assuming the systems are still bound, the orbital period of V4046 Sgr C[D] with respect to V4046 Sgr AB would be of order $\sim 10^6 \text{ yr}$, i.e., a significant fraction of their estimated ages. This system would therefore appear to be the most loosely bound hierarchical binary system known in the β PMG. However, two similarly loosely bound binaries have been identified thus far in the TWA: TWA 11AB and TWA 11C, projected separation $\sim 13500 \text{ AU}$ (Kastner et al. 2008a) and TW Hya (TWA 1) and TWA 28, projected separation $\sim 41000 \text{ AU}$ (Teixeira et al. 2008). The separations of these nearby, young hierarchical multiple systems are comparable to those of the most loosely bound binaries in the solar neighborhood (the separation distribution of nearby field binaries appears to be truncated at $\sim 20,000 \text{ AU}$; Close et al. 1990). The (very low-mass) TWA 30A and 30B star/disk systems, which are separated on the sky by $\sim 3400 \text{ AU}$ (Looper et al. 2010), are also very weakly bound.

However, the analysis in §2.2 strongly implies that V4046 Sgr AB and the putative V4046 Sgr C[D] could only be coeval if the latter, like the former, is a nearly-equal-components binary — consistent with previous suspicions concerning this system (Torres et al. 2006). Furthermore, if the two systems indeed formed together, then the position of V4046 Sgr C[D] in Fig. 1 appears to place a conservative lower limit of $\sim 8 \text{ Myr}$ on the age of the V4046

Sgr multiple system, while — on the basis of this comparison of V4046 Sgr C[D] with pre-MS tracks alone, and given the present uncertainties in the stellar parameters — the system may be as old as ~ 25 Myr.

Numerical simulations of hierarchical triple star systems demonstrate that the action of Kozai oscillations, in combination with tidal friction, shrinks and circularizes the orbit of the inner binary (Fabrycky & Tremaine 2007). Although Fabrycky & Tremaine (2007) find that the fraction of circularized, close (few-day period) binaries with tertiaries as distant as V4046 Sgr C[D] should be negligibly small, they also note that $\sim 40\%$ of hierarchical triple systems are “lost” from their numerical sample, due to dissolution. Perhaps V4046 Sgr AB and C[D] constitute such a (recently dissolved) hierarchical multiple system that, at a slightly earlier epoch, resembled closer, young hierarchical binaries (such as the ~ 8 Myr-old TWA systems HD 98800 and Hen 3-600). If so, the dissolution of V4046 Sgr AB and C[D] evidently occurred $\sim 10^6$ yr ago and left behind a close binary with a nearly circular orbit (V4046 Sgr AB has an eccentricity $e < 0.01$; Stempels & Gahm 2004).

Given that V4046 Sgr has apparently well outlived the “canonical” few-Myr timescale for Jovian planet formation (e.g., Currie et al. 2009, and references therein), one might further speculate that the presence of V4046 Sgr C[D] may explain the longevity of the circumbinary disk around V4046 Sgr AB — just as the hierarchical natures of the young multiple systems HD 98800 and Hen 3-600 may explain the persistence and observed properties of the circumbinary dust disk in each of these systems (see, e.g., Prato et al. 2001; Furlan et al. 2007; Andrews et al. 2010, and references therein). Although it remains to work out the details in all of these examples, in the specific case of V4046 Sgr it is possible that dynamical interactions with component(s) C[D] may have inhibited the formation of gas giant and ice giant planets in circumbinary orbits around components AB, thereby preserving the gaseous, circumbinary disk from which this close binary system is still accreting.

This research was supported by NASA Goddard Space Flight Center XMM-Newton Guest Observer Facility and NASA Astrophysics Data Analysis Program grants to RIT (NASA grant numbers NNX09AT15G and NNX09AC96G, respectively). DPH was supported by NASA through the Smithsonian Astrophysical Observatory (SAO) contract SV3-73016 for the Chandra X-Ray Center and Science Instruments. MA acknowledges support from the Swiss National Science Foundation (grants PP002-110504 and PP00P2-130188). The authors thank B. Zuckerman for useful discussions, the anonymous referee for a thorough and insightful review, and Emily Thompson (West Irondequoit [NY] High School) for contributions to the catalog research reported herein.

REFERENCES

- Akeson, R. L., et al. 2011, *ApJ*, 728, 96
- Andrews, S. M., Czekala, I., Wilner, D. J., Espaillat, C., Dullemond, C. P., & Hughes, A. M. 2010, *ApJ*, 710, 462
- Argiroffi, C., Maggio, A., Montmerle, T., et al. 2011, *ApJ*, submitted
- Baraffe, I., Chabrier, G., Allard, F., & Hauschildt, P. H. 1998, *A&A*, 337, 403
- Close, L. M., Richer, H. B., & Crabtree, D. R. 1990, *AJ*, 100, 1968
- Currie, T., Lada, C. J., Plavchan, P., Robitaille, T. P., Irwin, J., & Kenyon, S. J. 2009, *ApJ*, 698, 1
- da Silva, L., Torres, C. A. O., de La Reza, R., Quast, G. R., Melo, C. H. F., & Sterzik, M. F. 2009, *A&A*, 508, 833
- Donati, J.-F., Gregory, S.G., Montmerle, T., et al. 2011, *MNRAS*, in press
- Fabrycky, D., & Tremaine, S. 2007, *ApJ*, 669, 1298
- Furlan, E., et al. 2007, *ApJ*, 664, 1176
- Günther, H. M., Liefke, C., Schmitt, J. H. M. M., Robrade, J., & Ness, J. 2006, *A&A*, 459, L29
- Huenemoerder, D. P., Kastner, J. H., Testa, P., Schulz, N. S., & Weintraub, D. A. 2007, *ApJ*, 671, 592
- Hughes, A. M., Wilner, D. J., Andrews, S. M., Qi, C., & Hogerheijde, M. R. 2011, *ApJ*, 727, 85
- Kastner, J. H., Huenemoerder, D. P., Schulz, N. S., Canizares, C. R., Li, J., & Weintraub, D. A. 2004, *ApJ*, 605, L49
- Kastner, J. H., Zuckerman, B., & Bessell, M. 2008a, *A&A*, 491, 829
- Kastner, J. H., Zuckerman, B., Hily-Blant, P., & Forveille, T. 2008b, *A&A*, 492, 469
- Kenyon, S. J., & Hartmann, L. 1995, *ApJS*, 101, 117
- Kurucz, R. L. 1993, *VizieR Online Data Catalog*, 6039, 0

- Looper, D. L., Bochanski, J. J., Burgasser, A. J., Mohanty, S., Mamajek, E. E., Faherty, J. K., West, A. A., & Pitts, M. A. 2010, *AJ*, 140, 1486
- Marois, C., Macintosh, B., Barman, T., Zuckerman, B., Song, I., Patience, J., Lafrenière, D., & Doyon, R. 2008, *Science*, 322, 1348
- Peres, G., Orlando, S., Reale, F., & Rosner, R. 2001, *ApJ*, 563, 1045
- Prato, L., et al. 2001, *ApJ*, 549, 590
- Riaz, B., Gizis, J. E., & Harvin, J. 2006, *AJ*, 132, 866
- Rodriguez, D. R., Kastner, J. H., Wilner, D., & Qi, C. 2010, *ApJ*, 720, 1684
- Rosner, R., Tucker, W. H., & Vaiana, G. S. 1978, *ApJ*, 220, 643
- Sacco, G. G., Orlando, S., Argiroffi, C., Maggio, A., Peres, G., Reale, F., & Curran, R. L. 2010, *A&A*, 522, A55+
- Siess, L., Dufour, E., & Forestini, M. 2000, *A&A*, 358, 593
- Stempels, H. C., & Gahm, G. F. 2004, *A&A*, 421, 1159
- Teixeira, R., Ducourant, C., Chauvin, G., Krone-Martins, A., Song, I., & Zuckerman, B. 2008, *A&A*, 489, 825
- Testa, P. 2010, *Space Sci. Rev.*, 157, 37
- Torres, C. A. O., Quast, G. R., da Silva, L., de La Reza, R., Melo, C. H. F., & Sterzik, M. 2006, *A&A*, 460, 695
- Torres, C. A. O., Quast, G. R., Melo, C. H. F., & Sterzik, M. F. 2008, in *Handbook of Star Forming Regions, Volume II: The Southern Sky*, ed. B. Reipurth, p. 757
- Zacharias, N., et al. 2010, *AJ*, 139, 2184
- Zuckerman, B., Rhee, J. H., Song, I., & Bessell, M. S. 2011, *ApJ*, 732, 61
- Zuckerman, B., & Song, I. 2004, *ARA&A*, 42, 685

Table 1: GSC0739: PHOTOMETRY^a

B	V	R	I	J	H	K
14.14	12.78	12.13	10.64	9.44 (0.02)	8.77 (0.04)	8.54 (0.02)

a) Photometric data compiled from SIMBAD (sources: Tycho and UCAC3 catalogs, and Torres et al. 2006). Photometric uncertainties available only for 2MASS data.

Table 2: GSC0739: XMM X-RAY SPECTRAL FIT RESULTS^a

(obs. interval)	C^b (s ⁻¹)	N_H (10 ¹⁹ cm ⁻²)	T_1 (MK)	EM_1^c (10 ⁵² cm ⁻³)	T_2 (MK)	EM_2^c (10 ⁵² cm ⁻³)	L_x (erg cm ⁻² s ⁻¹)	$\log L_x/L_{\text{bol}}$
(1)	0.24	0.0–3.0	5.2–5.6	3.1–3.3	21–23	3.3–3.5	9.6×10^{29}	–2.76
(2)	0.12	2.0–8.0	5.3–5.8	2.4–2.6	17–20	1.1–1.3	3.8×10^{29}	–3.17
(3)	0.081	3.0 ^d	5.2–5.6	2.8–3.1	14–27	0.38–0.6	2.9×10^{29}	–3.28

NOTES: a) Fit to absorbed two-component, variable-abundance (APED) plasma models, with parameter ranges corresponding to 90% confidence intervals. b) Combined MOS1+MOS2 count rate. c) Plasma component emission measure. d) Parameter fixed during fitting.

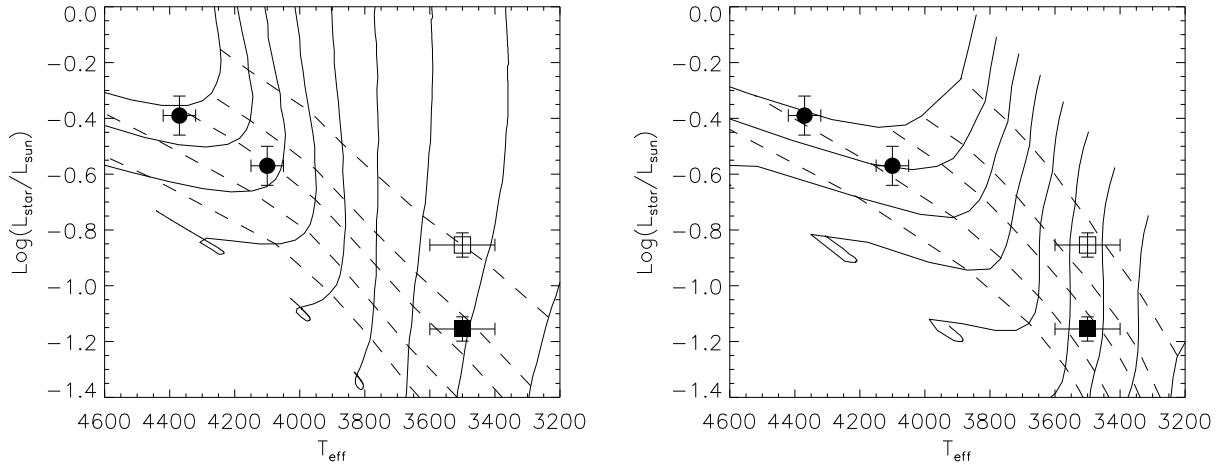


Fig. 1.— The HR diagram positions of V4046 Sgr AB (circles; luminosity and temperature data from Donati et al. 2011) and GSC0739 (squares; see §2.2) overlaid on pre-MS tracks from Siess et al. (2000, left panel) and Baraffe et al. (1998, right panel). The empty square indicates the observed position of GSC0739; the filled square indicates its position assuming it is a binary system composed of a pair of identical stars. In each panel, the evolutionary tracks (solid lines) correspond to masses ranging from 0.2 to 1.0 M_{\odot} (in intervals of 0.1 M_{\odot} , from right to left), while the isochrones (dashed lines) correspond to ages of 5, 10, 15, 25 and 40 Myr (from top to bottom).

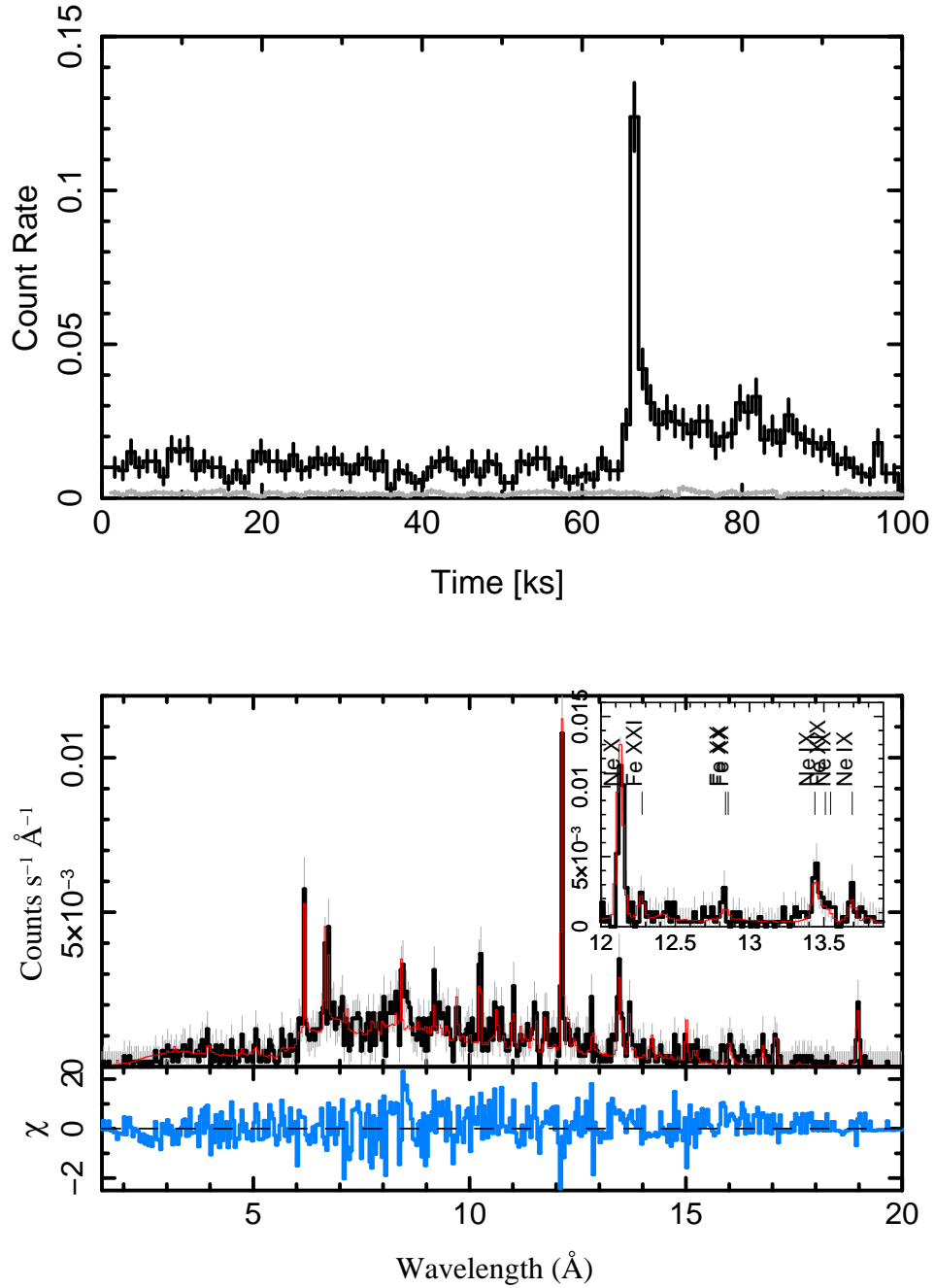


Fig. 2.— *Top*: Chandra/HETGS light curve of GSC0739, covering the longer (~ 100 ks) continuous observing segment of the two-segment 145 ks exposure. Black: source; grey: background. *Bottom*: Chandra/HETGS spectrum of GSC0739 (black, with grey error bars) overlaid with best-fit APED plasma model (red) in which the emission measure distribution is assumed to follow a power law (see text). The lower panel shows the residuals of the fit. The inset is a blowup of the 12.0–13.9 Å region, illustrating the strong emission lines of Ne x and Ne ix as well as weak lines of highly ionized Fe.

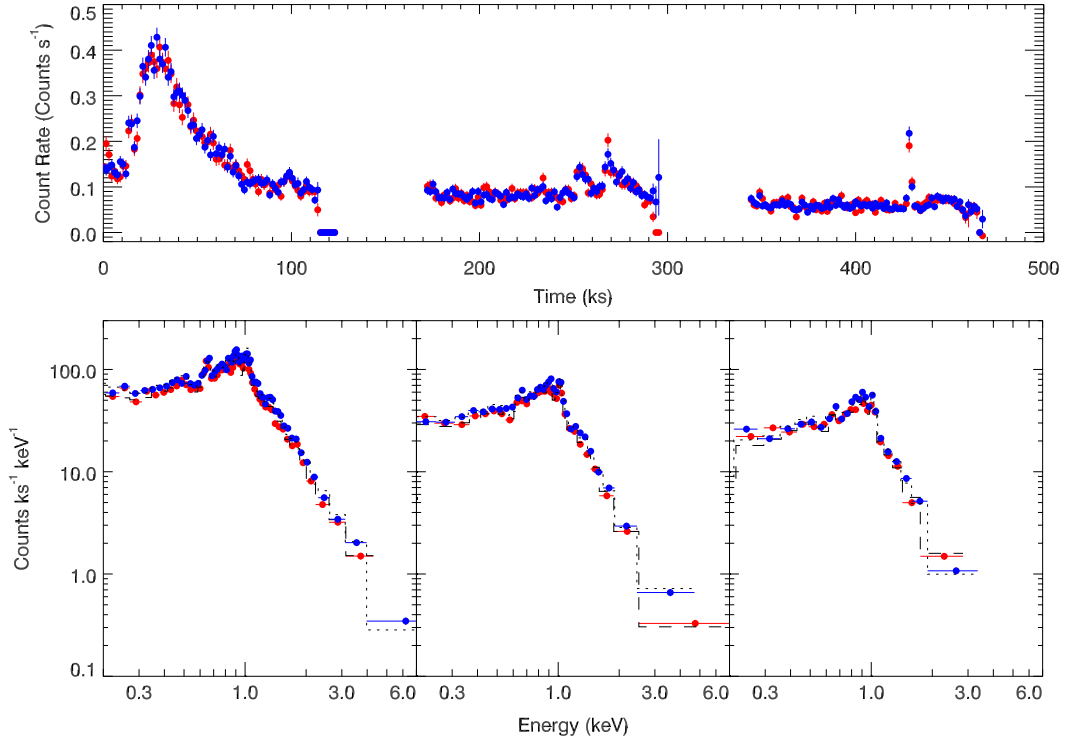


Fig. 3.— *Top*: XMM/EPIC MOS light curve of GSC0739. Binsize is 1500 s. *Bottom*: MOS spectra corresponding to the three ~ 100 ks observing intervals illustrated in the light curve in the top panel, with best-fit two-component thermal plasma models overlaid. In all panels, red points indicate MOS1 data and blue points indicate MOS 2 data.